Nano Energy (2015) 14, 226–235

Available online at www.sciencedirect.com

ScienceDirect

journal homepage: www.elsevier.com/locate/nanoenergy

RAPID COMMUNICATION

Human walking-driven wearable all-fiber triboelectric nanogenerator containing electrospun polyvinylidene fluoride piezoelectric nanofibers

Tao Huang[a], Cheng Wang[a], Hao Yu[a,*], Hongzhi Wang[b,*], Qinghong Zhang[c,*], Meifang Zhu[a]

[a]*State Key Laboratory for Modification of Chemical Fibers & Polymer Materials, College of Materials Science and Engineering, Donghua University, Shanghai, 201620, PR China*
[b]*Shanghai Key Laboratory of Functional Hybrid Materials, College of Materials Science and Engineering, Donghua University, Shanghai, 201620, PR China*
[c]*Engineering Research Center of Advanced Glasses Manufacturing Technology, College of Materials Science and Engineering, Donghua University, Shanghai 201620, PR China*

Received 28 November 2014; received in revised form 7 January 2015; accepted 24 January 2015
Available online 4 February 2015

KEYWORDS
Wearable nanogenerators;
Triboelectricity;
Electrospinning;
Polyvinylidene fluoride

Abstract
A simple-to-fabricate, high-performance, wearable all-fiber triboelectric nanogenerator (TENG)-based insole composed of electrospun piezoelectric polyvinylidene fluoride (PVDF) nanofibers sandwiched between a pair of conducting fabric electrodes that effectively harvests energy during human walking is reported. The surface of the nanofibers is roughened with secondary nanostructure to enhance insole performance. The maximum output voltage, instantaneous power and output current from the insole reach 210 V, 2.1 mW and 45 μA, respectively. The role of the piezoelectric effect in the electrospun PVDF nanofibers in this TENG-based insole is then systematically investigated. This device is shown to be a reliable power source that can be used to light up 214 serially connected light-emitting diodes directly. The soft fiber-based electric power generator demonstrated in this paper is capable of meeting the requirements of wearable devices because of its efficient energy-conversion performance, high durability, user comfort, and low cost.

*Corresponding authors. Tel.: +86 21 67792432.
E-mail addresses: yuhao@dhu.edu.cn (H. Yu), wanghz@dhu.edu.cn (H. Wang), zhangqh@dhu.edu.cn (Q. Zhang).

http://dx.doi.org/10.1016/j.nanoen.2015.01.038
2211-2855/

Introduction

The growing popularity of portable smart electronics and wearable electronic systems has stimulated interest in human motion-based energy-harvesting techniques because of a large development lag in the battery industry [1-3]. Harvesting the energy from bodily motion and other human activities offers strong potential to ensure the independent and sustainable operation of such systems without the use of a battery, or at least to extend the lifetimes of the batteries used [4-6]. It is in principle feasible that the energy harvested from bodily movements or the surrounding environment may be sufficient to support the working modes of nanoelectronic devices because of their extremely low power consumption [7-10]. To scavenge energy from mechanical movement, especially human activity, the study of wearable, sustainable electrical power generators that work at various frequencies and in various directions of deformation, and that are based on soft and durable materials, attracts considerable research. To realize this concept, fiber-based electric power generators are highly desirable because they are light and comfortable for users to wear. Flexible, soft fiber-based generators can be designed in such a manner that they are highly integrated with textiles such as items of clothing, trousers, or shoe insoles that people wear in daily life.

At present, two physical effects are being widely used to fabricate nanogenerators for converting low-level mechanical energy into electricity. Piezoelectric nanogenerators (PENGs) rely on the piezoelectricity that is driven by random mechanical motion [11-21]. For example, Lee et al. [22] reported a hybrid-fiber piezoelectric generator that converts low-frequency mechanical movements from human/animal activity into electricity. Meanwhile, Hwang et al. [23] demonstrated a flexible, highly efficient energy harvester consisting of a single-crystalline piezoelectric $(1-x)Pb(Mg_{1/3}Nb_{2/3})O_{3-x}PbTiO_3$ thin film on a plastic substrate to produce a self-powered artificial pacemaker with sufficient electric output current. The other physical behavior nanogenerators are often based on is the triboelectric effect. Triboelectric nanogenerators (TENGs) have recently been used to harvest mechanical energy from irregular vibrations, triggering, sliding, rotations, and even acoustic waves [16,19,24-29]. For PENGs, especially flexible ones, their typically low output power is a critical problem for wearable nanogenerators. Substrate materials such as polyethylene terephthalate (PET) or polydimethylsiloxane (PDMS) films have limited flexibility and breathability, which decreases the comfort of wearing such devices. The output powers of TENGs are much higher than those of most flexible PENGs, and are thus a better choice for harvesting mechanical energy where higher energies are needed.

To enhance the friction effect and enable production of a high-output generator, the fabrication of micro/nanostructures on the surfaces of triboelectric materials is required [30]. The methods that are currently used to design and fabricate these micro/nanostructures are based on photolithography [27,31-33] or reactive ion etching [28,34-36], and are both complicated and expensive. Therefore, the need for a simple, cost-effective, durable and readily scalable fabrication method to manufacture the surface structures of triboelectric materials should be addressed.

Electrospinning is a simple, low-cost and versatile method to produce ultrathin fibers from a rich variety of materials including polymers, composites, and ceramics [37,38]. Electrospun nanofibers show a number of unique properties, including one-dimensional morphology, extraordinary length, high surface area, and hierarchically porous structures. Modification of the solutions and processing parameters [39,40] or set-up geometry [41] allows complex nanostructures with controllable hierarchical features to be prepared, such as nonwoven, aligned or patterned fibers, nanoribbons, nanorods, random three-dimensional (3D) structures, nanonets and convoluted fibers with controlled diameters [42-46]. Furthermore, nanostructures can easily be formed on the surface of a single nanofiber; further increasing surface roughness, which is an important factor in improving the performance of TENGs. Another remarkable feature of electrospinning is that the structures can easily be prepared as membranes that can be conveniently handled and manipulated during application, which is especially important for sensors, and energy-conversion or storage devices [47-50]. Additionally, nanofiber membranes are lightweight, soft and have high porosity, which makes them suited for wearable devices when compared with the recently reported properties of dense polymer films and flexible rubbers [27,30,32,35]. Therefore, we believe that the use of nanofiber structures to improve the performance of TENGs may also lead to new design ideas for devices, particularly self-powered wearable electronics, which are both simple and cost-effective.

Here, we fabricate the first wearable insole-shaped TENGs that are composed of all-fiber structures, substrate-free and produce high output power by a simple electrospinning method. To achieve this objective, we explored several approaches in this research, including: (1) replacing the dense films that are traditionally used for such devices with high-porosity nanofiber nonwoven fabrics that are air permeable (average air permeability of 39.68 mm s^{-1}; see Supporting information, Figure S1), not only to meet the requirements for wearer comfort, but also to take advantage of the unique nanofiber structures of electrospun nonwoven fabrics, which offer large contact areas to enhance the friction effect to produce a high-output generator; (2) replacing the commonly used negative triboelectric materials PDMS and polytetrafluoroethylene, which have poor processability and are unsuitable to wear, with polyvinylidene fluoride (PVDF). PVDF was selected because it is readily processed to form nanofibers and possesses strong electronegativity according to the triboelectric series [51] (see Supporting information, Figure S2). In addition, secondary nanostructures could easily be fabricated on the surfaces of the PVDF nanofibers to increase the output performance of the TENG-based insole; (3) replacing the positive side triboelectric material films such as PET and polymethyl methacrylate, which easily lose electrons, with nickel- and copper-coated PET-conducting fabrics [51]. Thus, the developed fabrics serve two roles: the first is to act as the triboelectric material, which easily loses electrons, and the other is to act as the electrode of the TENG to collect signals. Therefore, the additional metal film electrode that is currently used in TENGs, and which shows a very short service lifespan under repeated mechanical deformation as well as poor wearability, is not required in

our device. The roughness of the fabric electrode also enlarges the friction effect, which further enhances the output power of the TENG-based insole.

Experimental

Materials

PVDF (FR904) was obtained from Shanghai 3F New Material Co., Ltd. N,N-Dimethylformamide (DMF, AR grade) and acetone (AR grade) were purchased from the Shanghai Chemical Reagent Plant. The conducting fabric (NF35D-C) used for the garment was purchased from Zhejiang Saint-year Electronic Technologies Co., Ltd. All materials were used without any further purification.

Electrospinning

PVDF was dissolved in a mixture of DMF and acetone (mass ratio of 6:4) at 80 °C to prepare a PVDF solution (10%, w/w). The homogeneous solution was then transferred into a plastic syringe for electrospinning. The electrospinning process was conducted in a custom-made setup, as shown in Figure 1, where the DC power supply was a JG50-1 Model HV power supply (Shanghai Shengfa Detection Instrument, China). In this experiment, the applied voltage was −20 kV. The spinning solution was drawn into a hypodermic syringe and delivered to the blunt needle tip at a flow rate of 1 mL h^{-1} using a microsyringe pump (KDS101, USA) at a fixed collection distance between the syringe tip and roller collector of 15 cm. Considering both the durability and wearability of the device, the roller collector was covered with a piece of wearable nickel- and copper-coated PET-conducting fabric rather than the alumina foil that is traditionally used. To enlarge the friction area and further enhance the output performance, secondary nanostructures were formed on the PVDF nanofiber surfaces carefully controlling the relative humidity between 40% and 50% during electrospinning. For comparison, PVDF nanofibers with smooth surfaces, *i.e.*, without secondary nanostructures, were also prepared by controlling the relative humidity below 30%. Both samples were prepared at a temperature of 23 ± 3 °C.

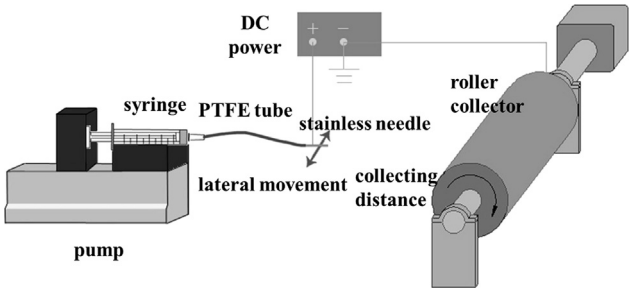

Figure 1 Schematic diagram of the custom-made electrospinning apparatus used in this experiment. The PVDF nanofibers were collected on the surface of a roller collector covered with conducting fabric.

Fabrication of the insole-based nanogenerator

First, a piece of the as-spun PVDF nanofiber (with the conducting fabric electrode) was sewn on the front of a piece of normal insole-shaped cloth. Then, an insole-shaped elastic sponge of the same size with hollowed-out regions at its front was sewn on the cloth above the PVDF nanofibers. Finally, another piece of conducting fabric, which was already sewn on a piece of cloth, was used to cover the elastic sponge to form a triboelectric material and also the fabric electrode.

Characterization

The air permeability of the TENG-based insole was tested using an automatic air permeability instrument (YG461H, China) according to a Chinese national standard (GB/T5453-1997). The morphology of the electrospun fibers was examined by field-emission scanning electron microscopy (FESEM, S-4800, Hitachi, Japan). A thin platinum layer was sputtered on the electrospun fiber surface before FESEM examination. The sheet resistance of the fabric electrode was measured by the four-point probe technique (Mitsubishi Chemical Holdings, MCP-T360). An oscilloscope (LeCroy, Wavesurfer 104MXs-B) was used to detect the output voltage of the insole while the human user was walking. The maximum current was measured under an external load of 500 kΩ. A Keithley 2000 m was used to measure the voltage across the capacitor during the charging process.

Results and discussion

Figure 2a shows a schematic diagram of the fabricated TENG-based insole. The PVDF nanofiber nonwoven fabric (bottom layer) and conducting fabric (top layer) were used to induce the triboelectric charge. To sustain these two layers and perform the charge generation and separation processes effectively, but without affecting the comfort of the wearer, a piece of insole-shaped elastic sponge of the same size with hollowed-out areas that acted as a spacer was inserted between the PVDF nanofibers and top layer of the conducting fabric. The working area of the TENG was approximately 6 × 5 cm^2. Figure 2b (1) and (2) are digital photographs of the as-spun PVDF nanofibers, which were firmly integrated with the conducting fabrics. The flexibility of the fabricated TENG-based insole is demonstrated in Figure 2b (3) and (4), which ensured its durability and wearability.

Operation of the insole-based TENG is realized by stepping on the top of the fabricated device so that the top layer of the conducting fabric is pressed periodically to make full contact with the PVDF nanofibers. When released, the two layers will separate and revert instantaneously back to their original shapes because of the highly resilient nature of the sponge layer. The working principle of the TENG is depicted schematically in Figure 2. In the original state, no electrical potential exists between the top layer of the conducting fabric and PVDF nanofibers, as shown in Figure 2c. By stepping on the insole, the insole is pressed such that the surfaces of the conducting fabric and PVDF nanofibers are charged with the same surface density [32], as illustrated in Figure 2d. When the force is removed, the

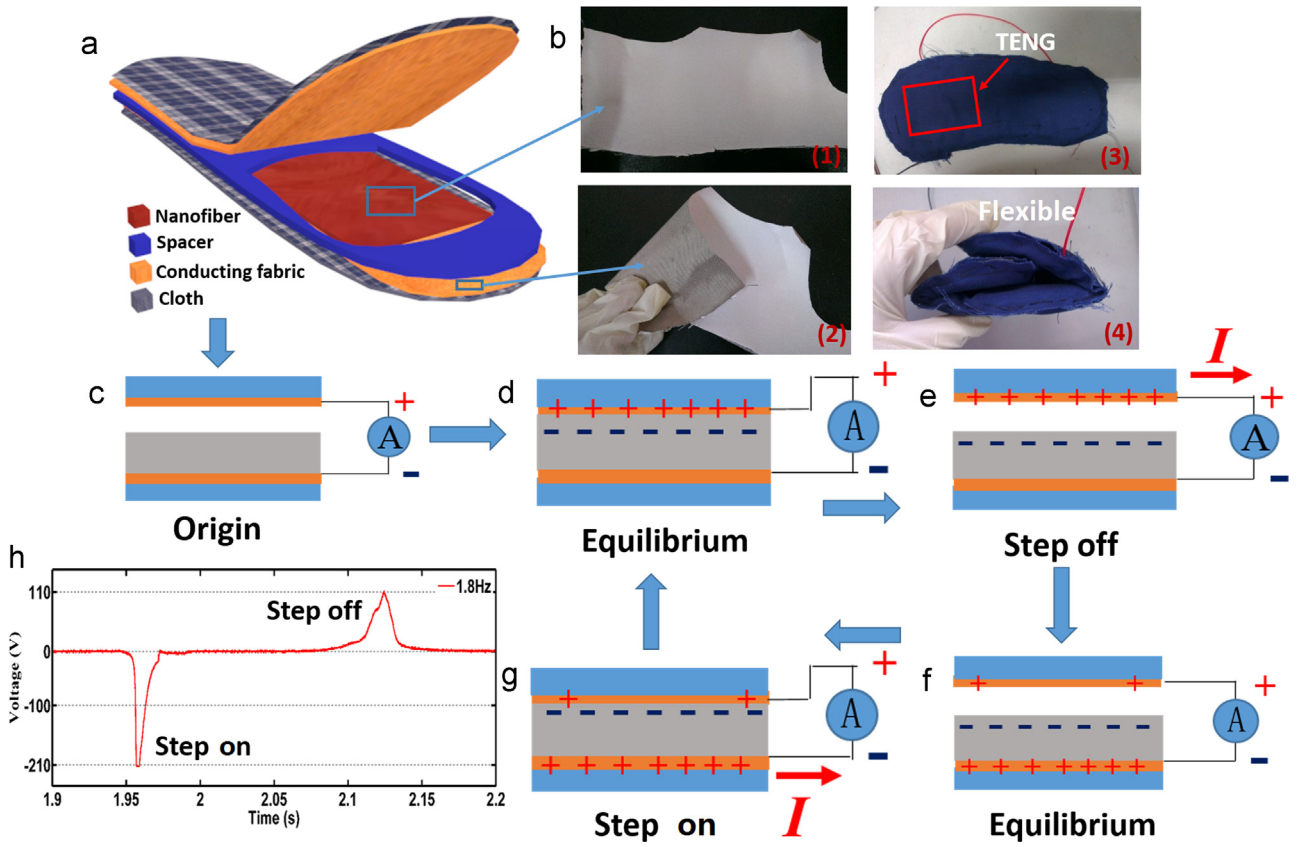

Figure 2 (a) Schematic diagram of the structure of the TENG-based insole; (b) digital photographs of the as-spun PVDF nanofibers on the conducting fabric (1) front side and (2) back side, (3) and (4) are photographs of the fabricated TENG-based insole demonstrating its flexibility. Working mechanism of the TENG when the device is in the states of (c) origin; (d) equilibrium; (e) step off; (f) equilibrium; (g) step on and (h) the corresponding voltage-time curve.

potential difference between the conducting fabric and PVDF nanofibers will drive the electrons in the bottom electrode to flow through the external circuit, which produces the observed current (Figure 2e), until the device reaches electrical equilibrium (Figure 2f). When the generator is pressed again, the redistributed charges will form a reversed potential, and thus drive the electrons to flow in the opposite direction (Figure 2g). The typical voltages generated by the insole that correspond to the step on/off states are presented in Figure 2h.

The electrical performance (Figure 3a) of the TENG-based insole with smooth PVDF nanofibers (Figure 3b) and Al flat electrode (Figure 3c) under the compressive force of human walking was investigated. The maximum output voltage generated by this device was 60 V at a frequency of 1 Hz. Compared with the performance of the cast dense PVDF films (Figure 3d and e) and Al flat electrode, the output voltage of the TENG-based insole with smooth PVDF nanofibers increased about tenfold. This is because the nanofiber structures increased the effective roughness to a greater degree than a flat PVDF film, and the friction surface area of the nanofibers was much larger than that of the bulk film.

To further enhance the electrical performance of the TENG-based insole, four groups of TENGs were fabricated, with (1) a fabric electrode and PVDF nanofibers with secondary nanostructure, (2) a flat Al electrode and PVDF nanofibers with secondary nanostructure, (3) a fabric electrode with smooth PVDF nanofibers, and (4) a flat Al electrode with smooth PVDF nanofibers, which are referred to hereafter as sample (1), (2), (3) and (4), respectively. These variations were then used to investigate the effects of PVDF nanofiber nanostructure and fabric electrodes on the output performance of the TENG-based insole, as shown in Figure 4a and b. (The measured output voltage and current curves under frequencies of 1 and 1.8 Hz are presented in Figures S3 and S4.) It is obvious that both the output voltage and current of these devices were enhanced by increasing the interface roughness of the friction surfaces. The use of nanofibers and a fabric electrode increased the effective roughness to a greater degree than a flat PVDF film and flat electrode. In addition, secondary nanostructures on the surfaces of the PVDF nanofibers were also fabricated to improve the performance of the TENG-based insole. The FESEM and 3D atomic force microscopy (AFM) images shown in Figure 4e and g, respectively, reveal that irregular ravine-like secondary nanostructures were formed on the nanofibers at a suitable solution evaporation rate, which was controlled through the humidity during electrospinning. Figure 4a indicates that the output voltage of sample (1) was increased by 66.7% and 75.0% at frequencies of 1 Hz (Figure S3a) and 1.8 Hz (Figure S3b), respectively, when compared with that of the corresponding values for sample (3) (shown in Figure S3e and S3f). Here, we must also note that the conducting fabric electrode, which also acted as one of the triboelectric materials, not only makes a major

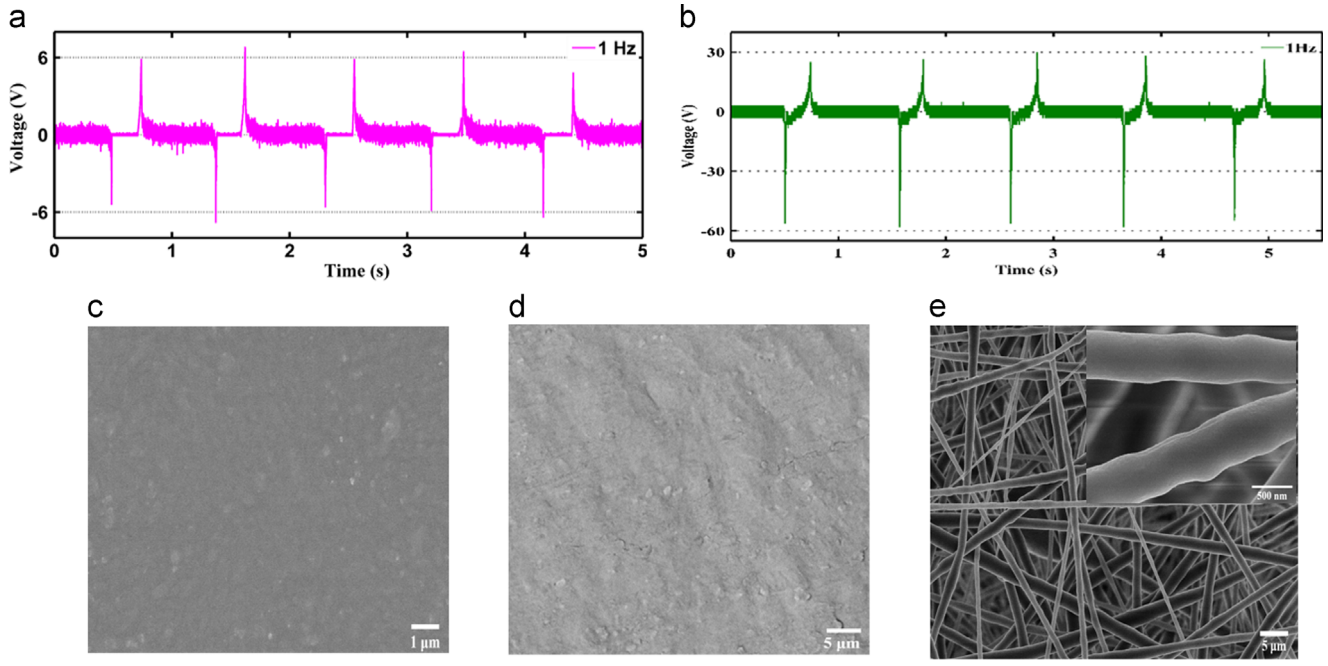

Figure 3 (a) Voltage generated by smooth PVDF nanofibers and Al flat electrode; (b) FESEM images of PVDF nanofibers. The inset shows a high-magnification image. (c) Al flat electrode; (d) voltage generated by the TENG-based insole with dense PVDF films and Al flat electrode and (e) SEM images of PVDF dense films.

contribution to the wearability and durability of the insole (the durability data for the output voltage of the TENGs are presented in Figure S5), but also played an important role in increasing the output voltage of the device because of its fiber structure. (We discuss the effect of the difference in triboelectric polarity between Al and Cu/Ni on the performance of the TENGs in the Supporting information, Figure S6.) Figure 4j shows the rough surfaces of the fabric electrode coated with Cu/Ni, which ensured its high conductivity. The sheet resistance of this electrode was $0.450 \pm 0.05\ \Omega\ sq^{-1}$ (high-magnification FESEM images and energy-dispersive X-ray spectroscopy data are provided in the Supporting information, Figure S7). The output voltage of sample (1) was increased by 15.4% and 16.7% at frequencies of 1 and 1.8 Hz, respectively, compared with the corresponding values for sample (2). Interestingly, the effects are more obvious when the PVDF nanofibers have smooth surfaces (*i.e.*, sample (3) and (4)), for which the output voltages increased by 60.0% at both 1 and 1.8 Hz for sample (3) compared with those for sample (4) (see Figure 4a). The variation of the currents is similar to that of voltages for the TENGs (Figure 4b).

The deformation frequency could also influence the output of the TENG. The maximum output voltage and current generated by the TENG-based insole with surface-nanostructured PVDF nanofibers under the compressive force of walking were 150 V and 22.5 μA at a frequency of 1 Hz, respectively. When the external frequency was increased to 1.8 Hz, which is equivalent to a common walking speed of 4 km h^{-1}, the output voltage and current increased to 210 V and 45 μA, respectively. This is because the external electrons flow to reach an equilibrium in a shorter time at faster walking speeds [32,52].

The energy generated by our TENG-based insole can be stored by connecting the device to a capacitor (2.2 μF) through a bridge circuit (see the inset of Figure 4c). The charging abilities of the four aforementioned TENGs are shown in Figure 4c, and reflect their output voltages. The cumulative charge can reach 1.9 μC in 10 steps by stepping on the insoles that are made of a fabric electrode and secondary-nanostructured PVDF nanofibers (sample (1)). The ladder-shaped charging curves clearly show the instantaneous generated charges that correspond to each individual step. The average instantaneous charges and direct current in a single step for charging the capacitor using sample (1) are 0.139 μC and 0.979 μA, respectively, which represent increases of 143.9% and 167.5%, respectively, when compared with the corresponding values for sample (4). (Detailed data are provided in the Supporting information, Table S8.)

PVDF nanofibers fabricated by electrospinning form a β phase with strong piezoelectricity (see the Supporting information, Figure S9) [52-54]. Compared with the reported PENGs containing electrospun PVDF nanofibers, the only difference between them and our TENGs is that for PENGs, the top electrode is firmly and directly attached to the PVDF nanofibers without any spacer so there is no relative shift between the fabric electrode and PVDF nanofibers. In PENGs, the role of the fabric electrode is only to collect the piezo-charges. Mechanical strain (the compression force as the insole is stepped on) can induce piezoelectric bound charges, which results in a built-in potential between the top and bottom surfaces of the nanogenerator. In response, the generated electrons can flow from the top electrode to the bottom electrode to neutralize this potential. When the strain is released as the foot is lifted off the insole, the built-in piezoelectric potential decreases and the electrons

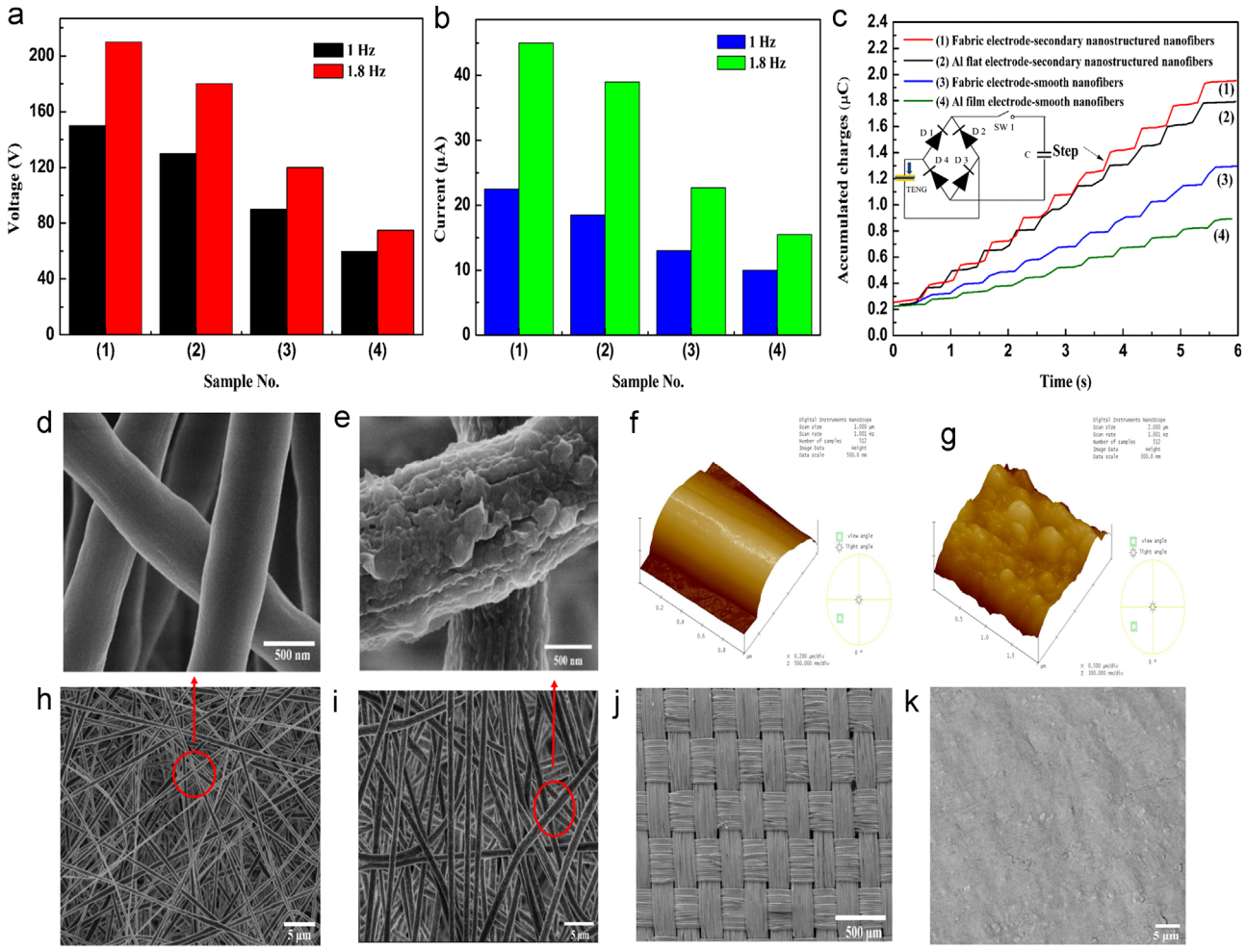

Figure 4 Characterization of the (a) output voltage; (b) current and (c) charging ability of the TENG-based insole with different structures, including (1) fabric electrode with secondary-nanostructured PVDF nanofibers, (2) Al flat electrode with secondary-nanostructured PVDF nanofibers, (3) fabric electrode with smooth PVDF nanofibers, (4) Al flat electrode with smooth PVDF nanofibers. Microstructures of (d) and(h) PVDF nanofibers with smooth surfaces; (e) and(i) secondary-nanostructured PVDF nanofibers. 3D AFM images of the (f) smooth and (g) rough surface of PVDF nanofibers. Microstructures of (j) fabric electrode and (k) Al flat electrode.

that have accumulated at the bottom electrode of the nanogenerator move back to the top side and then build up an electric pulse in the opposite direction (see the Supporting information, Figure S10) [19,55].

In contrast, the TENGs contain an elastic sponge with hollowed-out areas between the top electrode and nanofibers as a spacer. When the TENG-based insole was subjected to a compression force as it was stepped on, piezoelectric bound charges originating from piezoelectric PVDF were generated, as well as triboelectric charges that originated from PVDF and the fabric electrode because of the considerable difference of electronegativity between these two tribological materials (the conducting fabric is positively charged, while PVDF is negatively charged). Thus, the output voltage generated by the TENG containing piezoelectric PVDF nanofibers is probably a combination of piezoelectricity and triboelectricity. Therefore, an important question arises as to whether the piezoelectricity of the PVDF played a positive or negative role in the TENG-based insole. To answer this, we reversed the orientations of the dipoles of the PVDF nanofibers by changing the polarity of the spinning voltage from negative to positive. As depicted in Figure 5a and c, the direction of CF_2 dipoles is determined by the direction of the applied electric field during electrospinning, which was oriented perpendicular to the surface of the electrospun mats. As a result, when the direction of the applied electric field was reversed (from negative to positive), the direction of the dipoles would also be reversed, as well as the direction of the voltage generated by piezoelectricity, as illustrated in Figure 5d and e. In contrast, the direction of the voltage generated by triboelectricity would remain the same (see Figure 5b). Therefore, the overall output would be increased when the directions of piezoelectric and triboelectric output are the same; otherwise, it would be decreased. To detect the piezoelectric signal from the nanofiber membranes, a PENG was fabricated by sandwiching an as-spun PVDF nanofiber membrane between two conducting fabric electrodes. Finally, the whole sandwich structure was encapsulated with transparent one-sided adhesive tape to ensure there was no relative movement between

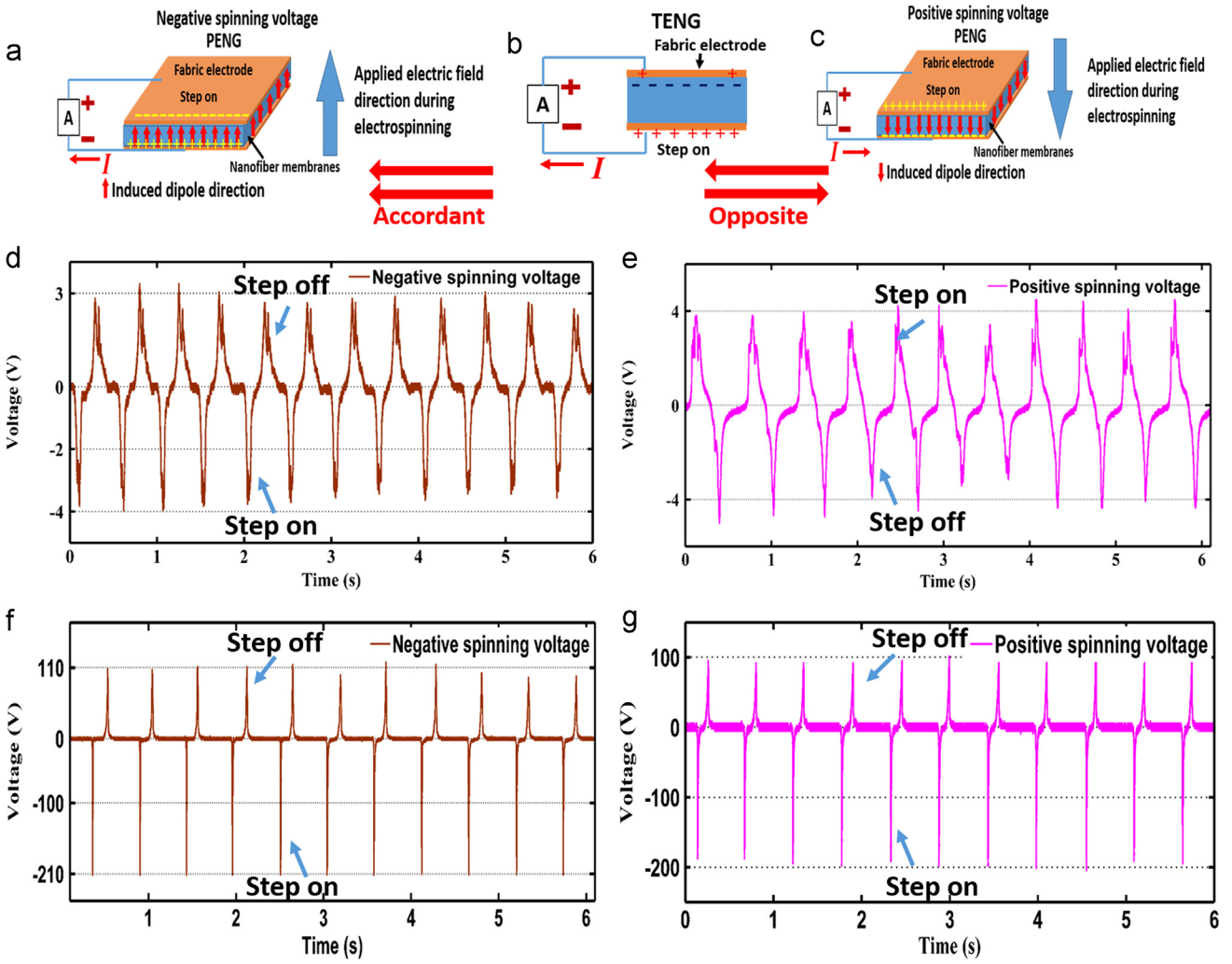

Figure 5 Schematic diagrams of (a) a PENG fabricated with negative spinning voltage; (b) a TENG fabricated by either negative or positive spinning voltage and (c) a PENG fabricated by positive spinning voltage. Voltage generated by piezoelectricity of PVDF nanofibers fabricated under (d) negative and (e) positive spinning voltage. Voltage generated by triboelectricity of PVDF nanofibers fabricated under (f) negative and (g) positive spinning voltage.

the fabric electrodes and nanofibers, so no triboelectric charges were generated in this case (this structure is similar to that reported by Zeng et al. [56]). Figure 5d and e shows the voltages generated by the piezoelectricity of the PVDF nanofibers fabricated under negative and positive spinning voltages, respectively. We can see that opposite voltages were generated under the same force direction because of the reversed orientations of the dipoles and the maximum output voltages are only 4 V. Figure 5f and g demonstrate the voltages generated by triboelectricity in the TENGs. Interestingly, the maximum voltage is increased from 200 to 210 V when the voltage direction is the same as that of the voltage generated by piezoelectricity. This indicates that the overall voltage is the sum of the voltages generated by piezoelectricity and triboelectricity. A positive contribution from piezoelectricity can be achieved by tuning its voltage direction in accordance with that of the triboelectricity by reversing the dipole direction.

In practice, there are generally two situations where energy-conversion devices such as PENGs or TENGs are used as power sources. The first is when the device is used to continuously provide energy for an energy-storage unit in a system, such as a lithium battery [57] or capacitor [58] as described above, where the energy can be stored for later use. The second case is where the energy is used instantaneously to directly drive small electronic devices such as light-emitting diodes [33] or medical devices [15]. In practical use, the output power for the load depends on the resistance of the load itself. Therefore, we determined the variations in output current and voltage of a working TENG-based insole (sample (1)) at a frequency of 1.8 Hz under different external loads from 500–1000 MΩ (Figure 6a). With an increase in load resistance, the current decreases, while the voltage exhibits the opposite behavior and saturates at a value of approximately 210 V, which is consistent with the output voltage of this device. The instantaneous power on the load reaches a maximum value of 2.1 mW at a load resistance of 8 MΩ (Figure 6b).

As a demonstration of the conversion of human walking-based energy into electricity to power an electronic device, our TENG-based insole was successfully used as a direct power source without any energy-storage system to instantaneously

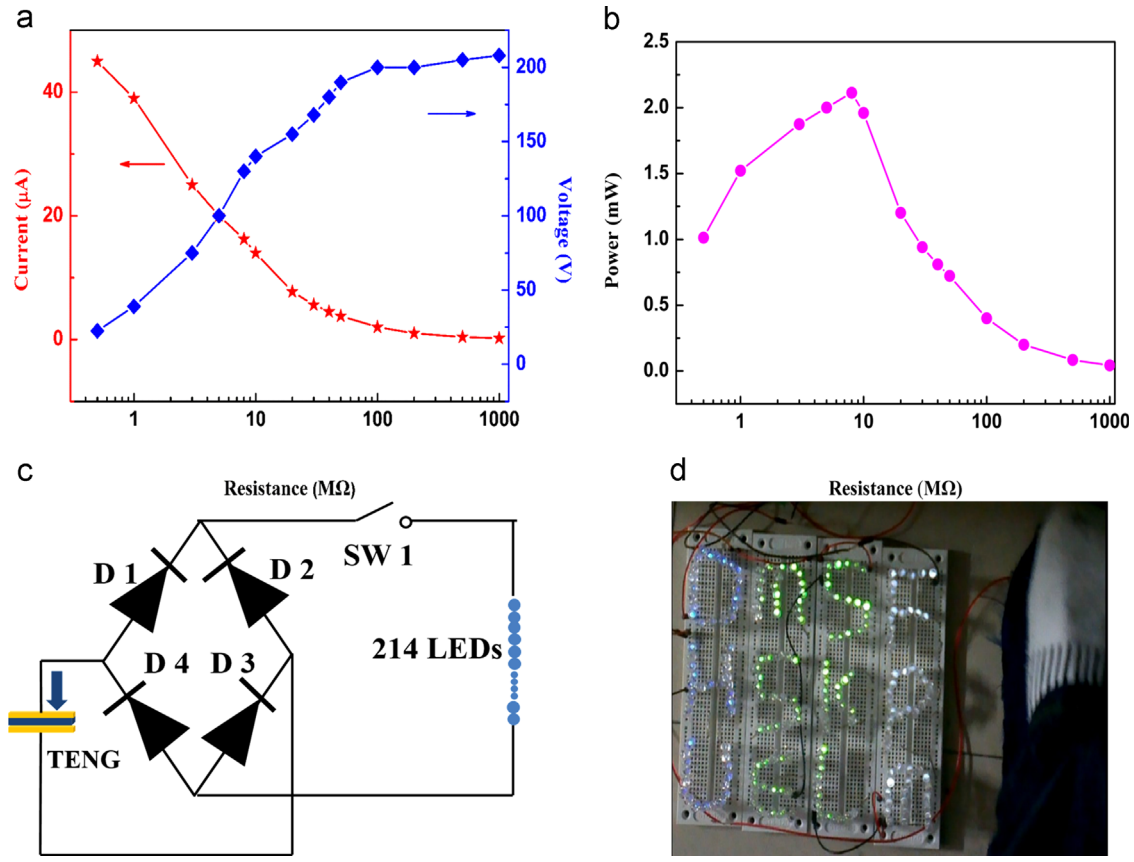

Figure 6 The dependence of the (a) output voltage, current, and (b) instantaneous power on load resistance. (c) Schematic diagram of the prototype energy-harvesting circuit and (d) a snapshot of flashing LEDs while directly stepping on the TENG-based insole.

power 214 commercial LEDs connected in series to form a character sequence of "DHU-MSE-SKL-PFM" by walking. Figure 6c and d shows a schematic diagram of the prototype energy-harvesting circuit and a photograph of the flashing LEDs when the TENG-based insole is being stepped on directly. A bridge rectifier is used to convert the AC output signals into DC signals (see the Supporting information, S11 Video 1).

Supplementary material related to this article can be found online at http://dx.doi.org/10.1016/j.nanoen.2015.01.038.

Conclusions

In summary, a wearable all-fiber structured TENG-based insole consisting of PVDF electrospun nanofibers and two conducting fabric electrodes that operates based on the triboelectric effect was developed. Nanofibers with rough surfaces were introduced to increase the friction areas and enhance the output performance of the device. The methods used here are much simpler and more cost-effective than those previously reported. The flexible conducting fabric electrode not only improves the wearability and durability of the insole, but also plays an important role in increasing the output voltage and current. The piezoelectricity generated by the PVDF nanofibers only increases the overall performance when the voltage direction of the piezoelectricity is the same as that of the triboelectricity. The TENG-based insoles were soft, flexible and lightweight; thus ensuring maximum comfort for the wearer, and were used to convert mechanical energy to light 214 LEDs connected in series simply by stepping force. We believe that the innovative approach demonstrated here could form a basis for new self-powered nanodevices that convert the low-frequency mechanical energy of human activity into electricity for applications such as implantable biomedical devices, wireless sensors, and wearable electronics.

Acknowledgment

We gratefully acknowledge the jointly financial support by the National Natural Science Foundation of China (No. 51473034), Specialized Research Fund for the Doctoral Program of Higher Education (20110075130001), Science and Technology Commission of Shanghai Municipality (12nm0503900, 13JC1400200), the Program for Professor of Special Appointment (Eastern Scholar) at Shanghai Institutions of Higher Learning, Innovative Reasearch Team in University (IRT1221) and the Program of Introducing Talents of Discipline to Universities (No.111-2-04), Chinese Universities Scientific Fund (CUSF-DH-D-2014029).

Appendix A. Supporting information

Supplementary data associated with this article can be found in the online version at http://dx.doi.org/10.1016/j.nanoen.2015.01.038.

References

[1] M.S. Dresselhaus, I.L. Thomas, Nature 414 (2001) 332–337.
[2] A.S. Arico, P. Bruce, B. Scrosati, J.-M. Tarascon, W. van Schalkwijk, Nat. Mater. 4 (2005) 366–377.
[3] Z.L. Wang, Adv. Funct. Mater. 18 (2008) 3553–3567.
[4] Z.L. Wang, J.H. Song, Science 312 (2006) 242–246.
[5] J.F. Scott, Science 315 (2007) 954–959.
[6] X. Wang, Nano Energy 1 (2012) 13–24.
[7] Z.L. Wang, Nanogenerators for self-powered devices and systems, Georgia Institute of Technology, SMARTech digital repository (2011) (http://hdl.handle.net/1853/39262).
[8] Y. Qin, X. Wang, Z.L. Wang, Nature 451 (2008) 809–813.
[9] Y. Li, F. Qian, J. Xiang, C.M. Lieber, Mater. Today 9 (2006) 18–27.
[10] J.A. Paradiso, T. Starner, IEEE Pervasive Comput. 4 (2005) 18–27.
[11] Y. Hu, L. Lin, Y. Zhang, Z.L. Wang, Adv. Mater. 24 (2012) 110–114.
[12] K.Y. Lee, B. Kumar, J.-S. Seo, K.-H. Kim, J.I. Sohn, S.N. Cha, D. Choi, Z.L. Wang, S.-W. Kim, Nano Lett. 12 (2012) 1959–1964.
[13] S. Min Kim, H. Kim, Y. Nam, S. Kim, AIP Adv. 2 (2012) 042174.
[14] G. Zhu, A.C. Wang, Y. Liu, Y. Zhou, Z.L. Wang, Nano Lett. 12 (2012) 3086–3090.
[15] X. Chen, S. Xu, N. Yao, Y. Shi, Nano Lett. 10 (2010) 2133–2137.
[16] L. Gu, N. Cui, L. Cheng, Q. Xu, S. Bai, M. Yuan, W. Wu, J. Liu, Y. Zhao, F. Ma, Y. Qin, Z.L. Wang, Nano Lett. 13 (2013) 91–94.
[17] K.-S. Hong, H. Xu, H. Konishi, X. Li, J. Phys. Chem. Lett. 1 (2010) 997–1002.
[18] K.-I. Park, M. Lee, Y. Liu, S. Moon, G.-T. Hwang, G. Zhu, J.E. Kim, S.O. Kim, D.K. Kim, Z.L. Wang, K.J. Lee, Adv. Mater. 24 (2012) 2999–3004.
[19] Z.-H. Lin, Y. Yang, J.M. Wu, Y. Liu, F. Zhang, Z.L. Wang, J. Phys. Chem. Lett. 3 (2012) 3599–3604.
[20] X.-Q. Fang, J.-X. Liu, V. Gupta, Nanoscale 5 (2013) 1716–1726.
[21] K.-I. Park, J.H. Son, G.-T. Hwang, C.K. Jeong, J. Ryu, M. Koo, I. Choi, S.H. Lee, M. Byun, Z.L. Wang, K.J. Lee, Adv. Mater. 26 (2014) 2514–2520.
[22] M. Lee, C.-Y. Chen, S. Wang, S.N. Cha, Y.J. Park, J.M. Kim, L.-J. Chou, Z.L. Wang, Adv. Mater. 24 (2012) 1759–1764.
[23] G.-T. Hwang, H. Park, J.-H. Lee, S. Oh, K.-I. Park, M. Byun, H. Park, G. Ahn, C.K. Jeong, K. No, H. Kwon, S.-G. Lee, B. Joung, K.J. Lee, Adv. Mater. 26 (2014) 4880–4887.
[24] Y. Hu, Y. Zhang, C. Xu, G. Zhu, Z.L. Wang, Nano Lett. 10 (2010) 5025–5031.
[25] G. Zhu, Z.-H. Lin, Q. Jing, P. Bai, C. Pan, Y. Yang, Y. Zhou, Z.L. Wang, Nano Lett. 13 (2013) 847–853.
[26] Q. Zhong, J. Zhong, B. Hu, Q. Hu, J. Zhou, Z. Wang, Energy Environ. Sci. 6 (2013) 1779–1784.
[27] X.-S. Zhang, M.-D. Han, R.-X. Wang, F.-Y. Zhu, Z.-H. Li, W. Wang, H.-X. Zhang, Nano Lett. 13 (2013) 1168–1172.
[28] Y. Xie, S. Wang, L. Lin, Q. Jing, Z.-H. Lin, S. Niu, Z. Wu, Z.L. Wang, ACS Nano 7 (2013) 7119–7125.
[29] J. Yang, J. Chen, Y. Liu, W.Q. Yang, Y.J. Su, Z.L. Wang, ACS Nano 8 (2014) 2649–2657.
[30] F.-R. Fan, Z.-Q. Tian, Z. Lin Wang, Nano Energy 1 (2012) 328–334.
[31] F.-R. Fan, L. Lin, G. Zhu, W. Wu, R. Zhang, Z.L. Wang, Nano Lett. 12 (2012) 3109–3114.
[32] S. Wang, L. Lin, Z.L. Wang, Nano Lett. 12 (2012) 6339–6346.
[33] W. Tang, B. Meng, H.X. Zhang, Nano Energy 2 (2013) 1164–1171.
[34] J. Chen, G. Zhu, W. Yang, Q. Jing, P. Bai, Y. Yang, T.-C. Hou, Z.L. Wang, Adv. Mater. 25 (2013) 6094–6099.
[35] G. Zhu, C. Pan, W. Guo, C.-Y. Chen, Y. Zhou, R. Yu, Z.L. Wang, Nano Lett. 12 (2012) 4960–4965.
[36] Y. Yang, H. Zhang, J. Chen, Q. Jing, Y.S. Zhou, X. Wen, Z.L. Wang, ACS Nano 7 (2013) 7342–7351.
[37] D. Li, Y.N. Xia, Adv. Mater. 16 (2004) 1151–1170.
[38] Y. Dzenis, Science 304 (2004) 1917–1919.
[39] S.A. Theron, E. Zussman, A.L. Yarin, Polymer 45 (2004) 2017–2030.
[40] N. Bhardwaj, S.C. Kundu, Biotechnol. Adv. 28 (2010) 325–347.
[41] W.E. Teo, S. Ramakrishna, Nanotechnology 17 (2006) R89–R106.
[42] M. Pokorny, V. Velebny, Rev. Sci. Instrum 82 (2011) 055112. http://dx.doi.org/10.1063/1.3592596.
[43] C. Ru, F. Wang, C. Ge, J. Luo, Rev. Sci. Instrum. 84 (2013) 086107. http://dx.doi.org/10.1063/1.4819123.
[44] D. Yang, B. Lu, Y. Zhao, X. Jiang, Adv. Mater. 19 (2007) 3702–3706.
[45] Y. Liu, X. Zhang, Y. Xia, H. Yang, Adv. Mater. 22 (2010) 2454–2457.
[46] J. Hu, X. Wang, B. Ding, J. Lin, J. Yu, G. Sun, Macromol. Rapid Commun. 32 (2011) 1729–1734.
[47] S.-H. Park, D.-H. Won, H.-J. Choi, W.-P. Hwang, S.-i. Jang, J.-H. Kim, S.-H. Jeong, J.-U. Kim, J.-K. Lee, M.-R. Kim, Sol. Energy Mat. Sol. Cells 95 (2011) 296–300.
[48] Y. Dai, W. Liu, E. Formo, Y. Sun, Y. Xia, Polym. Adv. Technol. 22 (2011) 326–338.
[49] S. Cavaliere, S. Subianto, I. Savych, D.J. Jones, J. Roziere, Energy Environ. Sci. 4 (2011) 4761–4785.
[50] A. Laforgue, J. Power Sources 196 (2011) 559–564.
[51] A.F. Diaz, R.M. Felix-Navarro, J. Electrostatics 62 (2004) 277–290.
[52] G. Cheng, Z.-H. Lin, L. Lin, Z.-l. Du, Z.L. Wang, ACS Nano 7 (2013) 7383–7391.
[53] H. Yu, T. Huang, M. Lu, M. Mao, Q. Zhang, H. Wang, Nanotechnology 24 (2013) 405401.
[54] J. Fang, X. Wang, T. Lin, J. Mater. Chem. 21 (2011) 11088–11091.
[55] C. Chang, V.H. Tran, J. Wang, Y.-K. Fuh, L. Lin, Nano Lett. 10 (2010) 726–731.
[56] W. Zeng, X.M. Tao, S. Chen, S. Shang, H.L.W. Chan, S.H. Choy, Energy Environ. Sci. 6 (2013) 2631–2638.
[57] X. Xue, P. Deng, S. Yuan, Y. Nie, B. He, L. Xing, Y. Zhang, Energy Environ. Sci. 6 (2013) 2615–2620.
[58] J. Fang, H. Niu, H. Wang, X. Wang, T. Lin, Energy Environ. Sci. 6 (2013) 2196–2202.

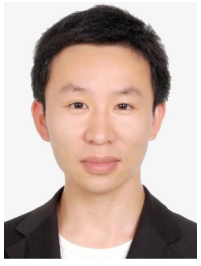

Tao Huang is a Ph.D. candidate in the College of Materials Science and Engineering, Donghua University, China and currently also a visiting Ph.D. student in the School of Aerospace, Mechanical and Mechatronic Engineering at the University of Sydney. His research interests mainly include functional polymer materials, structural analysis and characterization of nanomaterials, nanogenerator development.

Cheng Wang received his B.S. in Macromolecular Materials from Donghua University, China in 2012. Now he is a M.S. student in the College of Materials Science and Engineering of the Donghua University. His research mainly focuses on fabrication of triboelectric nanogenerators.

Prof. Hao Yu obtained his Ph.D. in 2003 from the Donghua University. Since 2013, he is a full professor in Donghua University. His main research focuses on triboelectric nanogenerators, modification of chemical fiber and electrospinning.

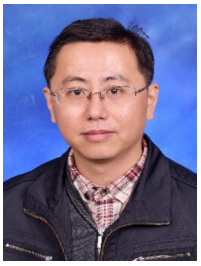

Prof. Hongzhi Wang obtained his Ph.D. in 1998 from the Shanghai Institute of Ceramics, Chinese Academy of Sciences. From 2000 to 2005, he was post-doctor at Microspace Chemistry Laboratory, National Institute of Advanced Industrial Science and Technology (AIST) in Japan. Since 2005, he is a full professor in Donghua University. His main research topics are devoted to (i) macroscopic-ordered graphene, (ii) luminescence materials for LED applications, (iii) structural color on fibers and (iv) electrochromic materials for smart windows.

Prof. Qinghong Zhang received his Ph.D. in 2000 from the Shanghai Institute of Ceramics, Chinese Academy of Sciences. From 2000 to 2008, he was assistant professor at Shanghai Institute of Ceramics, Chinese Academy of Sciences. Since 2008, he is a full professor and researcher at Donghua University. His main research focuses on new type of thin film solar cells, solar catalytic materials and organic-inorganic hybrid materials.

Prof. Meifang Zhu received her Ph.D. in 1999 from the Donghua University. Scince 2000 she is a full professor in Donghua University. Her main research topics are devoted to organic/inorganic hyrid materials and modification of chemical fibers.